

Correlation between the Bulk Flow Hydrodynamics, Wind Shear Stress and Evolution of the Surface Waves

Mamoun A. M. Janajrah^a*, Omar O. Badarn^b

^a*Mechatronics Engineering Department, Al-Balqa Applied University, P.O. Box 15008, Amman, Jordan*

^b*Mechanical Engineering Department, Al-Balqa Applied University, Amman, Jordan*

Abstract

Wind generated surface waves is described as being when the wind blows over the water surface and its momentum transfers through the surface to the bulk and generates perturbations throughout. The appearance of the surface waves starts if the disturbing effects due to the action of wind shear stress and induced bulk flow perturbations exceed the effect of restoring forces of gravity, capillary and viscous forces; this occurs as the flow transition from laminar to turbulent occurs. Based on the above description of wind generated surface waves the characteristics of the surface waves depend on strength of the induced bulk perturbations, wind shear stress and the physical properties of the surface. The correlation between evolution of the surface waves and the first two factors are discussed in this paper, however the effect of the physical properties of the water surface will be discussed in a separate paper. It was found that -irrespective of the wind speed -the waves cannot be generated under the effect of wind action until the strength of the induced bulk flow perturbations become significant and when the laminar-turbulent flow transition occurs. The evolution of the bulk flow parameters under effect of wind action (such as flow velocity, vorticity, swirling strength, shear strength, velocity vector angle) as the wind attains different orders were obtained using PIV system.

Keywords: *PIV, surface waves, flow hydrodynamics*

1. Introduction

The purpose of this research is to study the relationship between the hydrodynamics of the bulk flow under effect of low wind speed action and the surface wave generation mechanism. This can be achieved by analysing and interpreting the velocity fields of the bulk flow under effect of different wind speeds and observing the evolution of the surface wave. The corresponding parameters that affect the evolution of kinematics and dynamics of the bulk flow should be measured to explain the relationship between the wind speed and the bulk evolution.

To analyse the kinematics and dynamics of the bulk flow under effect of wind action, a group of experiments were conducted using water channel-wind tunnel facilities as described in experimental facilities section. The velocity fields measured using the PIV system, were produced after being processed using commercial software. The velocity fields were analysed and interpreted by converting the velocity field images to data using Tecplot software and a PIV commercial software

package (LaVision). The converted data are plotted against a position along the water channel in the direction of the wind. The most important parameters that can be extracted and converted to data from the velocity field images are flow velocity, velocity vector angle, vorticity, swirling strength and these parameters were plotted against a position along the water channel.

The velocity field images and movie sequences that captured and recorded at different wind speeds have given a good approach to understand the bulk flow evolution under the action of wind. This can be achieved by observing the following parameters at different wind speeds: the evolution of vortices statistics (size, strength), the direction of the flow with respect to wind direction at different depths from the surface and the velocity distribution through the bulk. Figure (1) shows one of the velocity field that measured using PIV system and processed using LaVision software.

* Corresponding author. Tel: +962 779820654

E-mail M_Janajrah@yahoo.com

© 2010 International Association for Sharing Knowledge and Sustainability

DOI:10.5383/ijtee.03.02.003

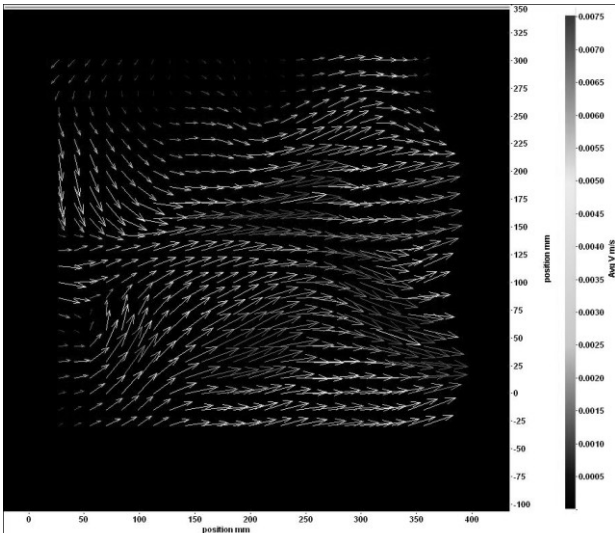


Fig (1) shows a velocity field measured using PIV system at a wind speed of the order 3.6 ms^{-1}

2. Experimental Facility

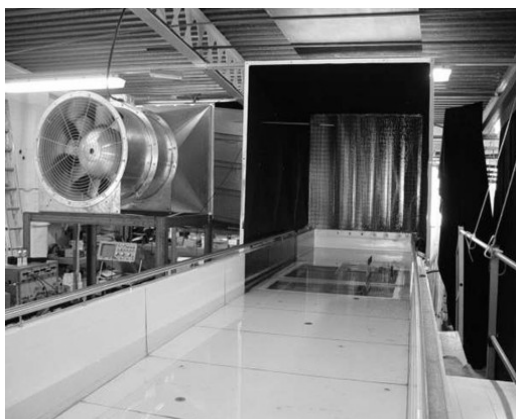
The experiments were conducted using the PIV system as a measurement system in a water channel of 9 m length, 1.22 m width, and 0.53m depth, fitted to a wind tunnel section transitioning smoothly over the water surface, in the Fluid Mechanics Laboratory at the University of Hertfordshire. The actual water depth was 0.45m. The fan speed was set at six

positions to change the wind speed. The wind speed was measured at a height of 1.22 m from the water surface where the fluctuations in the measured data are less as possible. At this height the effects of the water surface and the roof of the wind tunnel on the air flow stability is less than other heights. Hot wire (H.W) anemometry was used for measuring the wind speed. Measurements using the Hot wire techniques at the given location are given in Table (1). Since the PIV system requires spreading tracers through the water channel to be illuminated when the laser sheet passing through the flow; hollow glass spheres with diameters of 9-13 μm were used as tracers and were added to the water before conducting the experiments.

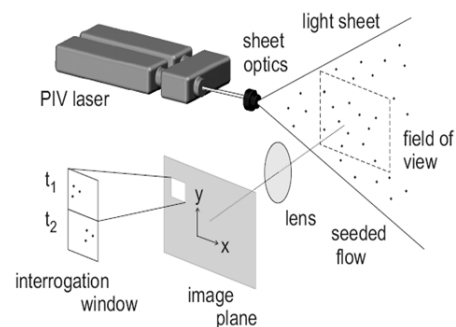
The 15Hz PIV system that used in our experiment includes: one 2M pixel camera, high resolution 2048 \times 2048, with the ability to control exposure time, triggering the image acquisition, and trigger schemes together with a 50 mJ double pulses YAGPIV laser. Commercial software (DaVis) was used to analyze the data. DaVis is a CCD image acquisition and processing program developed by LaVision. The double laser beam used to illuminate the spheres was sited under the water channel and the camera placed perpendicular to the laser sheet. In order to allow the laser sheet to traverse the water from the bottom to the surface and to capture instantaneous images, parts of the bottom and channel sides are made from glass. The PIV measurement zones were located at three fetch lengths from the upstream leading edge of the water channel.

Table 1. Wind speed measurements using Hot Wire t six positions of the fan motor input frequency

Fan motor Input Frequency (Hz)	0	10	20	30	40	50	0
$U_{1,2} \text{ ms}^{-1}$	0	1.07	1.92	2.73	3.6	4.5	0



Water channel and wind tunnel



Digital camera

Fig. (2) the experiment setup; water channel, wind tunnel, PIV laser and Digital camera

3. The hydrodynamic of the flow

In a bulk hydrodynamic formulation the momentum flux is related to the difference in mean wind speed between the surface and some height, z , using a dimensionless drag coefficient C_D

$$\frac{\tau}{\rho} = C_D [U_z - U_s]^2 = u_*^2 \quad (1)$$

Where U_z and U_s are the wind speed at height z from the surface and the surface velocity respectively. The correlation between the rate of momentum flux and the induced perturbation can be inferred from the evolution of the bulk flow parameters such as instantaneous velocity (flow velocity) V , Vorticity $Rot(z)$, Swirling strength S_w , and Velocity vector angle, α . These parameters attain higher magnitudes as the flow perturbations increase due to increasing the wind momentum that transfer to water bulk through the water surface. To explore the kinematics and dynamics of the flow under the effect of the wind action that blows steadily over the water surface at different speeds, the following properties of the flow that are extracted from the PIV measurements will be discussed and analysed separately.

- Average of instantaneous flow velocity fields, V_{avg}
- Velocity vector angle, α
- Vorticity, $Rot(z)$
- Swirling strength, S_w

To show more clearly the effects of the wind speed on the evolution of the bulk flow, the velocity field images were imported using Tecplot software to generate plots. The PIV measuring zone was located at (1.52) m from the upstream leading edge of the water channel, and the wind tunnel fan was set at six positions to generate wind with six different speeds.

4. Average of instantaneous flow velocity fields

The velocity fields were recorded at six different wind speeds for 19 seconds each. The average of the velocity of each recording was calculated as $V_{avg} = 1/n \sum_{i=1}^n V_i$ Figure (3) shows the relationship between the flow velocity and the position along the water channel at different wind speeds. The PIV measure was located at F1 and instantaneous flow velocity V_i s calculated according to the equation.

$$V_i = \sqrt{V_{xi}^2 + V_{yi}^2} \quad (2)$$

As shown in Figure (3) the flow velocity increases steadily when the wind speed increases from zero to 2.73 ms^{-1} . However, at wind speeds of 3.6 and 4.5m/s, the increase of flow velocity reaches a peak followed by rapid decay. This is in contrast with the lower wind speeds where a plateau may be seen. The maximal flow velocity occurs at the maximal wind speed whereas at low wind speeds the flow velocity is comparatively very low. This pattern reveals the evolution of the flow under the action of steady wind, which may help in understanding the relationship between the wind speed, surface wave generation and flow evolution. It is not possible to generate surface wind waves without introducing perturbations through the flow. These results confirm the prediction of an analytical model by Teixeira and Belcher (2006) ; the key stage in surface wave initiation may be immediately following laminar-turbulent transition of the flow, when the turbulence is not too anisotropic. They concluded that the turbulence in the water may be much more important for the initiation of surface waves than previously expected because the associated

pressure fluctuations are much more efficient. Also these results are consistent with the experimental results of Caulliez et al (1998) that were conducted in a laboratory, which supports the idea of ‘explosive wave’ - as they called it - after the transition of the flow to turbulence of shear current induced by the wind. Explosive waves describe the abrupt growth of the initial surface wave under the action of wind. The corresponding values of Reynolds number that scale the bulk flow regime for the results of Figure (3) are shown in Table (2). The appearance of the visible wave starts at a wind speed of 2.73 ms^{-1} and the corresponding Reynolds number at this speed indicates that the flow transition to turbulent occurs at this speed.

5. Velocity Vector Angle

Another parameter that can be extracted from the velocity fields and helps in understanding the kinematics and dynamics of the flow under the action of wind is the velocity vector angle α . The velocity vector angle describes the angular movement of the velocity vectors (tracers) with respect to an axis X parallel to the water surface. The PIV velocity fields revealed that the tracers have two types of movements translational (linear) and angular. In the first movement the tracers progress in different directions making a distance with respect to a reference point, where

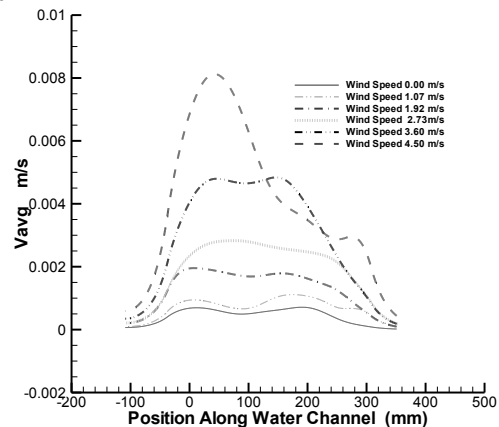


Fig. (3) Correlation between the wind speed and flow velocity along the water channel.

Table (2) shows the values of Reynolds number for the first and the second sets

Wind speed ms^{-1}	Reynolds Number (set one)
0	450
1.07	540
1.92	951
2.73	1406
3.6	2428
4.5	2880

in the angular movements the tracer's particles oscillate in an angular manner making an angle with respect to the reference X axis. The angle α was assumed positive in the direction of the wind and in the direction of the water surface. Figure (4-a) shows the correlation between the velocity vectors angles and the wind speed. The maximal velocity vector angles occur where the wind speed attains the minimal and maximal magnitudes. Firstly, the magnitude of velocity vector angle decays when the wind speed increases and the lesser magnitude

occurs at a wind speed of the order 2.73 ms^{-1} . Then the velocity vector angle grows to higher values at higher wind speeds. This sequence could be understood as a change in the movement of water particles from random movement in all directions at lower wind speeds to a confined movement following the direction of wind induced shear at higher speeds, or as the flow regime transition from laminar to turbulent. The purpose of analysing the velocity vector angle is to find a relationship between the flow pattern (laminar, transition and turbulent) and the magnitude of the velocity vector angle, and therefore a relationship between velocity vectors angles and the initiation of surface waves. An explosive growth of surface waves occurred after transition of the flow to turbulence of shear current induced by the wind as proved previously by experimental and analytical work. Based on such investigations, the parameter used to scale the flow regime transition from laminar to turbulent can be used to scale the transition of water surface from undisturbed surface to fully developed wave. Since the velocity vector angle is a function of wind and flow velocity, it is suggested that this parameter is used to scale such a transition. A visible surface wave was observed when the wind speed was 2.73 ms^{-1} . The shear current induced by the wind was insignificant when the wind speed less than of 2.73 ms^{-1} . It is supposed that the laminar - turbulence transition occurs in the flow - in the current measurements - as the magnitude of velocity vector angle attains the minimal magnitude. At this angle the water particle movements translate from random behaviour to directed movement by the induced wind shear and vortices. In these conditions the surface waves start to be visible. Figure (4-b) illustrates the relationship between the velocity vector angle (α) and the water height (h_w). The water height was measured from the bottom of the channel and was divided into seven sections. The difference between the min-max velocity vector angles at each section for six different wind speeds was recorded and plotted against the water height. At the first section near the bottom (0-30mm) the magnitude of, α , fluctuates between 13° - 45° for all wind speeds except for the wind speed of 3.6 ms^{-1} which was 98° . Broadly, α , is a function of wind speed and water height. For example, at the wind speed of the order 0 and 1.07 ms^{-1} , α grows as the h_w increases and the maximal α magnitude occurs at h_w of the order 230 mm and 280 mm (approximately at middle depth of the water channel) for the two speeds respectively then α decays to different magnitudes. At speed of 1.92 and 2.73 ms^{-1} α obtains low magnitudes and fluctuates over a small range as h_w increases. The magnitude of α fluctuations increase at a speed of the order 3.6 ms^{-1} . However, at a speed of 4.5 ms^{-1} α shows exponential growth with respect to h_w . The correlation between the maximal fluctuations in magnitude of α and the wind speed is shown in Figure (4-c). The minimal fluctuations in magnitude of α occur at the wind speeds of 1.92 and 2.73 ms^{-1} which gives another confirmation for the above results. The other interpretation of the behaviour of α may be attributable to the wind-water interaction mechanism. It is suggested that the wind particles attract and repel the water particles due to the electrostatic charges that accumulate on both of them. The repulsion and attraction processes may cause an angular motion for the water particles under the 'still' water conditions and at very low wind speed action. However, under the effect of higher wind speed action, the wind induced shear gradually exceeds the repulsion and attraction forces. The water particles follow the direction of the induced shear and which causes a reduction in α magnitudes. At a higher wind speed the magnitudes of α increase due to the induced shear and vortices formation and propagation. This interpretation may help in understanding the wave generation mechanism

when the surfactants or contaminants on the on the water surface disrupt the wave initiation and growth under the action of low wind speed. The surfactants and contaminants initiate a lamina (barrier) between the air and the water surface and eliminate the particles attraction and repulsion forces between the charged particles that distributed randomly in

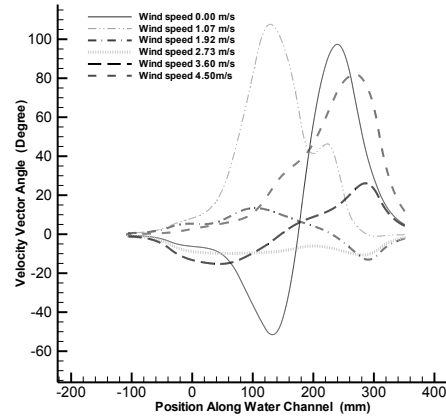


Fig. (4-a) Correlation between the wind speed and velocity vector angle along the water channel

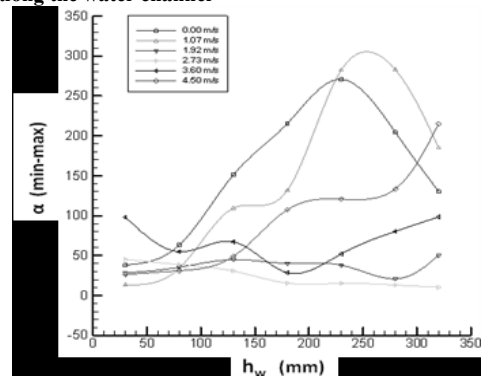


Fig (4-b): Correlation between the maximal difference of the angle α and water depth

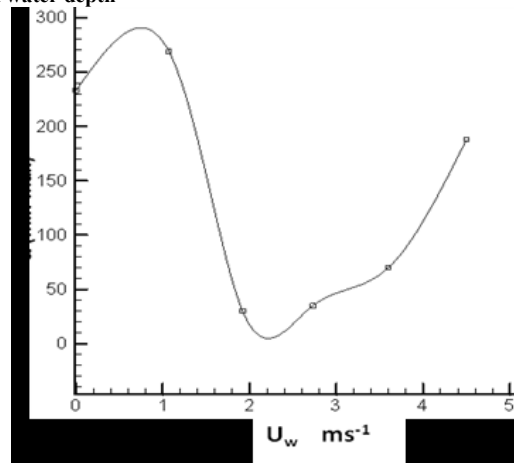


Fig. (4-c): Correlation between the maximal difference of the angle α and wind speed

the air and water bulk. In this case the contaminants shield the water from the effect of wind action which makes the two flows of water and wind independent from each other. In this case the wave generated by the effect of the mechanical action only whereas the other actions (thermal and chemical) are put out of action. A higher wind is required to producing and growth surface waves as observed in our experiments and in Kahma and Donelan (1988) observations.

6. Vorticity

The vorticity analysis is generally used to identify location of vortices and to calculate the vortex statistics (size, strength, etc). The possibility of forming stronger, larger and faster vortices increases as the vorticity attains higher magnitudes. It has been surprisingly challenging for the fluid dynamics community to arrive at a consensus definition of a vortex or an eddy, Adrian (2000).The definition offered by Kline and Robinson (1989) ‘a vortex exists when an instantaneous stream line mapped into a plane normal to the force exhibits a roughly circular or spiral pattern, when viewed in a reference frame moving with the centre of the vortex core’. According to Adrian (2000), a key condition in this definition is that the velocity field must be viewed in a frame that moves at the same velocity as the core of the vortex. A second condition is that the vorticity is concentrated in a core. Unfortunately, vorticity not only identifies the vortex core but also any shearing motion present in the flow, Adrian (2000). Vorticity is defined as

$$Rot(z) = \nabla \times V \tag{4}$$

The symbol ∇ can be used to describe the curl (rotational motion at points in a fluid). The vector product operation can be visualised as a pseudo-determinant:

$$\nabla \times V = \begin{vmatrix} i & j & k \\ \frac{\partial}{\partial x} & \frac{\partial}{\partial y} & \frac{\partial}{\partial z} \\ u & v & k \end{vmatrix} x \ y \ z$$

The vorticity $Rot(z)$ in current measurements determines the two dimensional vorticity in the xy-plane. The rotation of the vectors fields is calculated according to the equation (3). Vorticity is calculated by simple central differences in the measured velocity components.

$$Rot(z) = E_{xy} - E_{yx}$$

$$Rot(z) = \frac{\partial u}{\partial y} - \frac{\partial v}{\partial x} \tag{3}$$

Vx component (u): Extracts the u – component of the velocity vector
Vy component (v): Extracts the v – component of the velocity vector

Fig (5) shows the relationship between the vorticity versus position along the water channel at different wind speeds. The vorticity has attained positive and negative values based on the direction of rotation - positive for clockwise rotation (following the direction of the wind). When the wind speed increased from approximately zero to 1.07ms⁻¹ the direction of rotation did not change and the vorticity attained a less values. The vorticity increased when the wind speed increased if the main vortices kept the same direction of rotation and decreased if the direction of rotation changed. A significant increase in vorticity occurred at wind speeds of the order 3.6 ms⁻¹ and 4.5 ms⁻¹ where a significant increase occurred in Reynolds number and in the ratio of the water-wind kinetic energy density. The relationship between the existing vortices and surface wave was observed by Volino & Smith (1999); the wave became visible to the naked eye as the vorticity magnitude became significant. However, insight into the wind-waves generation and evolution mechanism can be obtained from observing the evolution of the vorticity; the existence of large and strong scale vortices may indicate the existence of high energy waves. So the parameters that affect the vortices’ formation and evolution may affect the formation and evolution of the waves in the same way. For instance, in shallow water, the friction induced by the water body bottom confines the evolution of the vortices’ size and speed which in turn confines wave evolution; only low amplitude waves with limited wavelengths can be

generated on shallow water surfaces even if the wind speed is significantly high. This is an example of one of the factors constraining the growth of the wave’s amplitude in shallow or short fetch water bodies. The correlation between the statistics of surface waves (amplitude, wave length, steepness, etc) and vortex statistics (size, strength, etc) should be considered under high wind speed in a water channel with different depths in further experiments. It is concluded that analysis of vortex statistics could provide a guide to predicting the surface wave’s statistics and vice versa.

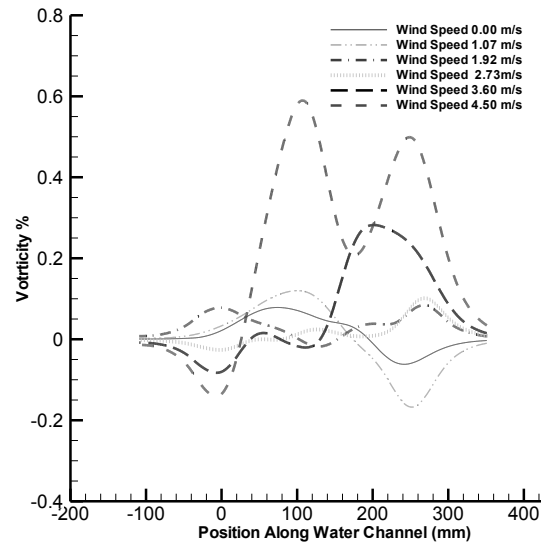


Fig. (5),Correlation between the wind speed and vorticity along the water channel.

7. Swirling Strength

Swirling strength is a parameter indicating a location around which the streamlines are closed, which is typically the location of the vortex core. According to Adrian et al (2000) Swirling strength is noted at all locations where a vortex was identified, and the swirling strength is more useful as a means of identifying eddies and calculating reliable vortex statistics than vorticity. This is because the vorticity is much noisier than the swirling strength and tends to identify local shear layers present in the field. The swirling strength in Figure (6) is determined by computing the eigenvalues of the velocity gradient centre. The critical point analysis of the local velocity gradient tensor and its corresponding eigenvalues have been proposed by several groups such as Zhou et al(1996,1999) in order to extract the underlining structure from velocity fields. In three dimensions, the local velocity gradient tensor will have one real eigenvalue (λ_r) and pair of complex conjugate eigenvalues ($\lambda_{ci} \pm i\lambda_{ci}$) when discriminant of its characteristics equation is positive. According to Chong et al (1990), when this is true the particles trajectories about the eigenvector corresponding to (λ_r) exhibit a swirling, spiral motion. λ_{ci}^{-1} represents the period required for a particle to swirl once about the λ_r axis. Thus $\lambda_{ci} > 0$ corresponds to shorter, more circular ellipse (eddies). Zhou et al (1996, 1999) showed that the strength of any local swirling motion is quantified by λ_{ci} , which they defined as the swirling strength of the vortex. Adrian et al (2000) reported, in two dimensions, that the local velocity gradient tensor will have two real eigenvalues or a pair of complex conjugate eigenvalues. Therefore, vortices are easily identified when $\lambda_{ci} > 0$. The algorithm of (6) is used in

the current measurements to calculate the swirling strength from the velocity field.

$$\max(0, \frac{\partial u}{\partial y} \frac{\partial v}{\partial x} - \frac{\partial u}{\partial x} \frac{\partial v}{\partial y}) \quad (5)$$

$$E_{xx} = \frac{\partial u}{\partial x}, \quad E_{yy} = \frac{\partial v}{\partial y}$$

then

$$\max(0, -(\frac{\partial u}{\partial y} \frac{\partial v}{\partial x} - \frac{\partial u}{\partial x} \frac{\partial v}{\partial y})/2 + (\frac{\partial u}{\partial x} \frac{\partial u}{\partial x} + \frac{\partial v}{\partial y} \frac{\partial v}{\partial y})/4)$$

i.e. only the positive part of the swirling strength λ_{ci} . The rest is set to zero to display swirl only.

In practice, high levels of swirling strength indicate the location of the vortex core. As shown in Figure (6), the swirling strength values at wind speeds less than 3.6 m/s are insignificant. A noticeable increase in the swirling strength values occurs at wind speeds of 3.6 ms⁻¹ and 4.5 ms⁻¹. These results do not match very well with Adrian's observations particularly at low wind speeds where the swirling is insignificant compared to the vorticity as shown in Figures (5 & 6). It is important to consider how the bulk flow is driven; for example Adrian analysed the PIV velocity fields that were measured in the radial plane of a fully developed turbulent pipe flow, whereas the current measurements were conducted in a semi opened water channel under the action of wind. The difference between the characteristics of the flow when the flow is driven by the action of wind or by mechanical means such as a circulation pump was observed in particular experiments conducted in two channels. In the first one, the flow is driven by the action of the wind and in the second the flow is driven by the action of the circulation pump. To find the difference between the two flows a small amount of dye was injected into both channels from the surface. When the flow was driven by wind action the dye followed the wind shear that was concentrated near the surface, whereas the dye was distributed across the channel from the surface to the bottom when the flow was driven by a circulating pump. This also may justify the difference between the characteristics of the surface waves that are generated by mechanical vibrator and by those generated by the action of the wind. Pierson et al (2003) have exposed two types of surface wave in opposition to the wind: one generated by mechanical vibrator and the other generated by wind action. They reported that the waves generated by mechanical vibrator collapsed faster than the other. The difference between the two cases may refer to the type of motion that was generated in the flow field by the action of the vibrator and or under the action of the wind. The latter introduces motion into the entire flow field whereas the former introduces a local motion depending on the location of the vibrator. Many studies concerning the surface wave generation under action of wind surface, for instance, Lorenz et al (2005) and Ataktürk and Katsaros (1998), discarded cases at wind speeds of less than 3 ms⁻¹ because the measurement systems of wave parameters did not show any significant response when wind speed was less than 3 ms⁻¹. The intimate relationship between the characteristics of the surface wave and kinematics and dynamics of the bulk is evident. As shown in Figure (5 & 6), up to wind speeds of 2.73 m/s the transfer of wind momentum to the bulk is not sufficient to initiate a detectable value of swirling strength and significant vorticity. For these reasons, in current measurements the waves cannot be observed at wind speeds less than 2.73 m/s. This value is not absolute, as it depends on the other parameters related to the water body and atmospheric conditions

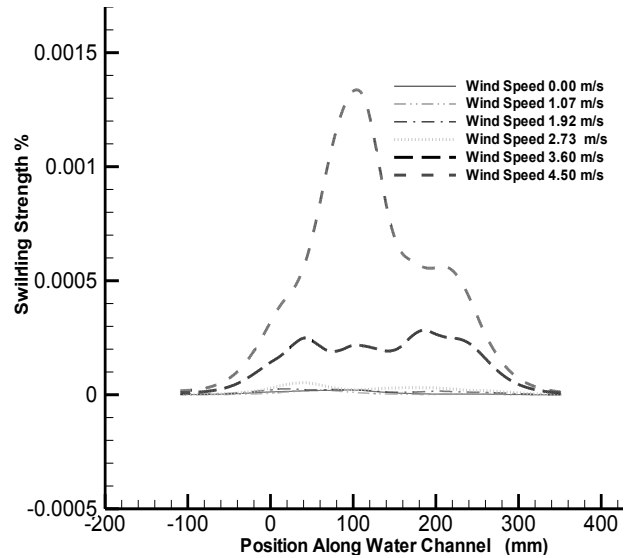


Fig. (6) Correlation between the wind speed and swirling strength along the water channel

8. Conclusion

The effect of the wind speed on the bulk flow parameters can be categorized depending on its behaviour into four groups:

1. Parameters which are affected by the action wind gradually from still water to a speed of the order 2.73 ms⁻¹. After that, an abrupt growth occurs in the maximum values at higher speeds. An example of this is the flow velocity.
2. Parameters, for instance the velocity vector angle, which are attained their maximal values at very low speeds and at the maximal wind speeds. The trend of the plots of this parameter tends to be similar to cosine wave form.
3. Parameters which are not affected by the wind action until a speed of 2.73 ms⁻¹. After that an abrupt growth in magnitude of these parameters occurs. Example of this: swirling strength.
4. Parameters which show little effect from the wind action until the speed of the order 2.73 ms⁻¹, after which an abrupt growth in these parameters occurs, for instance: vorticity.

The waves attain energy from the wind that is blowing over the surface and from the vortices that propagate towards the surface. In the absence of one of these sources, the waves become weak and tend to attenuate. The parameters that may affect the growth of the vortices' size and strength, such as water depth and wind speed, affect also the growth of the surface waves. This gives insight into the intimate relationship between the characteristics of the surface waves and the characteristics of the bulk under the action of wind.

References

- [1] Adrian, R.J. Christensen, K.T. Liu, Z.C., "Analysis and interpretation of instantaneous turbulent velocity fields", *Experiments in fluid*, 2000, 29, (275-290)
- [2] Atakürk, S.S, and, Katsaros, K.B., "Wind stress and surface waves observed on lake Washington", *Journal of physical oceanography*, 1999, 29, 633-650. [http://dx.doi.org/10.1175/1520-0485\(1999\)029<0633:WSASWO>2.0.CO;2](http://dx.doi.org/10.1175/1520-0485(1999)029<0633:WSASWO>2.0.CO;2)
- [3] Caulliez, G., Ricci N., and DuPont R., "The generation of the first visible wind waves", *Physics fluids* 1998,10, 757-759. <http://dx.doi.org/10.1063/1.869600>
- [4] Kahma, K.K., and, Donelan, M.A., , "A laboratory study of the minimum wind speed for wind wave generation", *J. Fluid Mech.* (1988) 192, 339-364. <http://dx.doi.org/10.1017/S0022112088001892>
- [5] Kline SJ, Robinson SK, "Quasi-coherent structures in the turbulent boundary layer", *Proceeding of Zaric Memorial Conference*, 1989, 200-217.
- [6] Lorenz, R.D., Kraal E.R., Eddlemon, E.E., Cheney, J., and Greeley, R., "Sea-surface wave growth under extraterrestrial atmospheres: Preliminary wind tunnel experiments with application to Mars and Titan", *ICARUS*, 2005, 175, 556-560. <http://dx.doi.org/10.1016/j.icarus.2004.11.019>
- [7] Pierson, W.L.,. Gracia A.W., and, Pells, S.E., "Water wave attenuation due to opposite wind", *J. Fluid Mech.*, 2003, 487 345-365. <http://dx.doi.org/10.1017/S0022112003004750>
- [8] Teixeira, M.A.C and, Belcher, S.E., "On the initiation of surface waves by turbulent shear flow", *Dynamics Atmospheres and Ocean*, 2006, 41, 1-27. <http://dx.doi.org/10.1016/j.dynatmoce.2005.10.001>
- [9] Volino R.J., Smith G. B., "Use of simultaneous IR temperature measurements and DPIV to investigate thermal plumes in a thick layer cooled from above", *Experiments in fluid* 1999, 27, 70-78.
- [10] Zhou J, Adrian RJ, Balachandar S, Kendall TM "Autogeneration of near wall vortical structure in channel flow", *Physics Fluid*, 1996, 8,288-290. <http://dx.doi.org/10.1063/1.868838>
- [11] Zhou J, Adrian R, Balachandar S, Kendall T, Mechanism for generation coherent packets of hairpin vortices in channel flow", *Fluid Mechanic*, 1999, 378, 353-359. <http://dx.doi.org/10.1017/S002211209900467X>